

The Relativistic Green's Function Model for Quasielastic Neutrino-Nucleus Scattering

C. Giusti¹, A. Meucci¹,

¹Dipartimento di Fisica, Università degli Studi di Pavia and INFN, Sezione di Pavia, via Bassi 6 I-27100 Pavia, Italy

Abstract. A model based on the relativistic impulse approximation (RIA) for quasielastic (QE) lepton-nucleus scattering is presented. The effects of the final-state interactions (FSI) between the emitted nucleon and the residual nucleus are described by the relativistic Green's function (RGF) model where FSI are treated consistently with the exclusive scattering and using the same complex optical potential. The results of the model are compared with the results of different descriptions of FSI and with available data for neutrino-nucleus scattering.

1 Introduction

A deep understanding of neutrino-nucleus cross sections is very important for the determination of neutrino oscillation parameters. Reliable models are required where all nuclear effects are well under control. Within the QE kinematic domain, the nuclear response to an electroweak probe is dominated by one-nucleon processes, where the scattering occurs only with the nucleon which is emitted and the remaining nucleons of the target behave as spectators. The process can adequately be described in the RIA by the sum of incoherent processes involving only one nucleon scattering. The components of the hadron tensor are then obtained from the sum, over all the single-particle (s.p.) shell-model states, of the squared absolute value of the transition matrix elements of the single-nucleon current. A reliable description of FSI between the emitted nucleon and the residual nucleus is a crucial ingredient for a proper description of data. The relevance of FSI has been clearly established for the exclusive $(e, e' p)$ reaction, where FSI are described in the nonrelativistic or relativistic distorted-wave impulse approximation (DWIA or RDWIA) using a complex optical potentials (OP) whose imaginary part gives an absorption that reduces the calculated cross section [1–7]. In the optical model the imaginary part accounts for the fact that in the elastic nucleon-nucleus scattering, if other channels are open besides the elastic one, part of the incident flux is lost in the elastically scattered beam and goes to the inelastic channels which are open. In the exclusive $(e, e' p)$ reaction, where the emitted proton is detected in coincidence with the scattered electron and the residual nucleus is left in a specific discrete eigenstate, only the selected channel contributes and it is correct to account for the flux lost

in the considered channel. In the inclusive scattering, where only the scattered lepton is detected and the final nuclear state is not determined, all elastic and inelastic channels contribute, the flux lost in a channel must be recovered in the other channels, and in the sum over all the channels the flux can be redistributed but must be conserved. A model based on the DWIA, where the cross section is obtained from the sum over all integrated one-nucleon knockout channels and FSI are described by a complex OP with an absorptive imaginary part, does not conserve the flux and it is conceptually wrong.

Different approaches have been adopted within the RIA to describe FSI in the inclusive QE lepton-nucleus scattering. In the relativistic plane-wave impulse approximation (RPWIA) the plane-wave approximation is assumed for the emitted nucleon wave function and FSI are simply neglected. In some RIA calculations FSI are incorporated in the emitted nucleon states by using real potentials, either retaining only the real part of the relativistic OP (rROP) or using the same relativistic mean-field potential considered in the description of the initial nucleon state (RMF) [8–10, 18, 19].

In the RGF model FSI are described in the inclusive scattering consistently with the exclusive scattering by the same complex ROP, but the imaginary part is used in the two cases in a different way and in the inclusive scattering the flux, although redistributed in all the channels, is conserved [11–25]. The Green’s function model was originally developed within a nonrelativistic and then a relativistic framework for the inclusive electron scattering. But for some differences and complications due to the Dirac matrix structure, the formalism follows within both frameworks the same steps and approximations. Relativity is, however, important at all energies, in particular at high energies, and in the energy regime of many neutrino experiments a relativistic model is required, where not only relativistic kinematics is considered, but nuclear dynamics and currents operators are described within a relativistic framework. Therefore only the relativistic RGF model has been extended to neutrino-nucleus scattering.

The RGF model and its results are reviewed in this contribution.

2 The Green’s Function Model

In the one-boson exchange approximation the cross section for QE lepton-nucleus scattering is obtained from the contraction between the lepton tensor, which in the plane-wave approximation for the lepton wave functions depends only on the lepton kinematics, and the hadron tensor $W^{\mu\nu}$, whose components are given by products of the matrix elements of the nuclear current J^μ between the initial and final nuclear states, *i.e.*,

$$W^{\mu\nu}(\omega, q) = \overline{\sum_i} \sum_f \langle \Psi_f | J^\mu(q) | \Psi_i \rangle \langle \Psi_i | J^{\nu\dagger}(q) | \Psi_f \rangle \times \delta(E_i + \omega - E_f), \quad (1)$$

where ω and q are the energy and momentum transfer, respectively.

For the inclusive scattering the diagonal components of the hadron tensor can equivalently be expressed as

$$W^{\mu\mu}(\omega, q) = -\frac{1}{\pi} \text{Im} \langle \Psi_i | J^{\mu\dagger}(q) G(E_f) J^\mu(q) | \Psi_i \rangle, \quad (2)$$

where $E_f = E_i + \omega$ and $G(E_f)$ is the Green's function, the full A-body propagator, which is related to the many body nuclear Hamiltonian. A similar but more cumbersome expression is obtained for the non-diagonal components [14].

The A-body Green's function in Eq. (2) defies a practical evaluation. Some approximations are required to reduce the problem to a tractable form. With suitable approximations, which are basically related to the IA, the components of hadron tensor can be written in terms of the s.p. optical-model Green's function. This result has been derived by arguments based on multiple scattering theory [26] or by means of projection operators techniques [11–14]. In the latter framework, the matrix element in Eq. (2) is decomposed into the sum

$$\text{Im} \langle \Psi_i | J^{\mu\dagger} G J^\mu | \Psi_i \rangle \sim A \sum_n \text{Im} \langle \Psi_i | j^{\mu\dagger} G_n j^\mu | \Psi_i \rangle, \quad (3)$$

where

$$G_n = P_n G P_n, \quad P_n = \int d\mathbf{r} | \mathbf{r}; n \rangle \langle n; \mathbf{r} | \quad (4)$$

is the projection of the full Green's function onto the channel subspace spanned by the orthonormalized set of states $| \mathbf{r}; n \rangle$, corresponding to a nucleon at the point \mathbf{r} and to the residual nucleus in the state $| n \rangle$. G_n is the the Green's function associated with the OP Hamiltonian which describes the elastic scattering of a nucleon by the $(A - 1)$ -nucleus in the state $| n \rangle$. The sum over n includes discrete eigenstates and resonances embedded in the continuum [11, 12].

The approximation in Eq. (3) has been derived neglecting non-diagonal terms $P_n G P_m$ and retaining only the one-body part j^μ of the current operator. It is basically a s.p.approach where one assumes that j^μ connects the initial state $| \Psi_i \rangle$ only with states in the channel subspace spanned by the vectors $| \mathbf{r}; n \rangle$, *i.e.*, only with states asymptotically corresponding to single-nucleon knockout. However, not only these states, but all the allowed final states are included in the inclusive response, as G_n in Eq. (4) contains the full propagator G : all the allowed final states are taken into account by the OP, in particular by its imaginary part.

The complexity of an explicit calculation of G_n can be avoided by means of its spectral representation, which is based on a biorthogonal expansion in terms of the eigenfunctions of the non-Hermitian OP and of its Hermitian conjugate [11, 12]. In the s.p. representation one obtains

$$W^{\mu\mu}(\omega, q) = \sum_n \left[\text{Re} T_n^{\mu\mu}(E_f - \varepsilon_n, E_f - \varepsilon_n) \right. \\ \left. - \frac{1}{\pi} \mathcal{P} \int_M^\infty d\mathcal{E} \frac{1}{E_f - \varepsilon_n - \mathcal{E}} \text{Im} T_n^{\mu\mu}(\mathcal{E}, E_f - \varepsilon_n) \right], \quad (5)$$

where \mathcal{P} denotes the principal value of the integral, n is the eigenstate of the residual nucleus with energy ε_n , and

$$\begin{aligned} T_n^{\mu\mu}(\mathcal{E}, E) = & \lambda_n \langle \varphi_n | j^{\mu\dagger}(\mathbf{q}) \sqrt{1 - \mathcal{V}'(E)} | \tilde{\chi}_{\mathcal{E}}^{(-)}(E) \rangle \\ & \times \langle \chi_{\mathcal{E}}^{(-)}(E) | \sqrt{1 - \mathcal{V}'(E)} j^{\mu}(\mathbf{q}) | \varphi_n \rangle. \end{aligned} \quad (6)$$

In Eq. (6) $\tilde{\chi}_{\mathcal{E}}^{(-)}$ and $\chi_{\mathcal{E}}^{(-)}$ are eigenfunctions, belonging to the eigenvalue \mathcal{E} , of the s.p. OP and of its hermitian conjugate, φ_n is the overlap between $| \Psi_i \rangle$ and $| n \rangle$, *i.e.*, a s.p. bound state, and the spectroscopic factor λ_n is the norm of the overlap function. The factor $\sqrt{1 - \mathcal{V}'(E)}$, where $\mathcal{V}'(E)$ is the energy derivative of the OP, accounts for interference effects between different channels and justifies the replacement in the calculations of the Feshbach OP \mathcal{V} by the local phenomenological OP

Disregarding the square root correction, the matrix elements in Eq. (6) are of the same type as the DWIA ones of the exclusive $(e, e'p)$ reaction, but both eigenfunctions $\tilde{\chi}_{\mathcal{E}}^{(-)}$ and $\chi_{\mathcal{E}}^{(-)}$ of $\mathcal{V}(E)$ and of $\mathcal{V}^\dagger(E)$ are considered. In the exclusive scattering the imaginary part of the OP accounts for the flux lost in the channel n towards the channels different from n , which are not included in the exclusive process. In the inclusive response, where all the channels are included, this loss is compensated by a corresponding gain of flux due to the flux lost, towards the channel n , in the other final states asymptotically originated by the channels different from n . This compensation is performed by the first matrix element in the right hand side of Eq. (6), which involves the eigenfunction $\tilde{\chi}_{\mathcal{E}}^{(-)}$ of the Hermitian conjugate OP, where the imaginary part has an opposite sign and has the effect of increasing the strength. Therefore, in the RGF model the imaginary part of the OP redistributes the flux lost in a channel in the other channels, and in the sum over n the total flux is conserved. The RGF model allows to recover the contribution of non-elastic channels starting from the complex OP that describes elastic nucleon-nucleus scattering data and provides a consistent treatment of FSI in the exclusive and in the inclusive scattering.

3 Results

The RGF model has been applied to the inclusive QE electron scattering and charged-current QE (CCQE) neutrino-nucleus scattering. Some numerical results are presented and discussed in this Section.

In all the calculations the bound nucleon states are self-consistent Dirac-Hartree solutions derived within a relativistic mean-field approach [27]. Different parameterizations for the ROP have been used: the energy-dependent and A-dependent EDAD1 [28] and the more recent democratic (DEM) [29] parameterizations, which are global parameterizations obtained through a fit to elastic proton-scattering data over a wide range of nuclei, and the energy-dependent but A-independent EDAI complex phenomenological potential [28]. While EDAD1

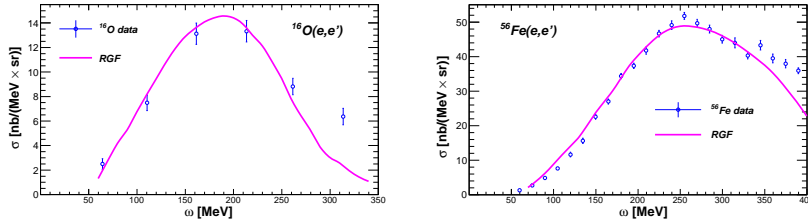


Figure 1. Differential cross sections of the reactions $^{16}\text{O}(e, e')$ (beam energy $\varepsilon = 1080$ MeV and scattering angle $\vartheta = 32^\circ$) and $^{56}\text{Fe}(e, e')$ ($\varepsilon = 2020$ MeV and $\vartheta = 20^\circ$) calculated in the RGF-DEM. Experimental data from [30] (^{16}O) and [31] (^{56}Fe).

and DEM depend on the atomic number A , EDAI is constructed only to fit elastic proton-scattering on a specific nucleus, for instance on ^{12}C , which is of particular interest for recent neutrino experiments.

The RGF model is in many cases able to give a reasonable description of the experimental (e, e') cross sections in the QE region, in particular in kinematic situations where the longitudinal response gives the main contribution. A numerical example is shown in Figure 1, where the RGF results are compared with the experimental (e, e') cross sections on ^{16}O and ^{56}Fe . The shape followed by the RGF results fits well the slope shown by the data, in particular approaching the peak region, where the calculated cross sections are in reasonable agreement with the data. Although satisfactory on general grounds, the comparison with data cannot be conclusive until contributions beyond the QE peak, like meson exchange currents and Δ effects, which may play a significant role in the analysis of data even at the maximum of the QE peak, are carefully evaluated.

The results of the RGF and RMF models have been compared for the inclusive QE electron scattering in [18] and for CCQE neutrino scattering in [19]. Both models can describe successfully the behavior of electron scattering data. There are, however, some differences which increase with the momentum transfer. The RMF model uses as input the real, strong, energy-independent, relativistic mean field potential that reproduces the saturation properties of nuclear matter and of the ground state of the nuclei involved. As such, it includes only purely nucleonic contribution and does not incorporate any information from scattering reactions. In contrast, the RGF, which uses as input a complex energy-dependent phenomenological ROP, incorporates information from scattering reactions and takes into account not only direct one-nucleon emission, but all the allowed final states. The imaginary part of the ROP includes the overall effect of the inelastic channels, which give different contributions at different energies. The differences between the RGF and RMF results can therefore be ascribed to the inelastic contributions which are incorporated in the RGF but not in the RMF, such as, for instance, re-scattering processes of the nucleon in its way out of the nucleus, non-nucleonic Δ excitations, which may arise during nucleon

propagation, as well as to some multinucleon processes. These contributions are not included explicitly in the model, but can be recovered by the imaginary part of the ROP. The comparison between the RGF and RMF results can therefore be useful to evaluate the relevance of inelastic contributions.

In the comparison with data, we may expect that the RGF can give a better description of the experimental cross sections which receive significant contributions from non-nucleonic excitations and multi-nucleon processes. This is expected to be the case [20, 32] of MiniBooNE CCQE data. While in electron-scattering experiments the beam energy is known and the cross sections are given as a function of the energy transfer, in neutrino experiments the energy and momentum transfer are not known and calculations are carried out over the energy range which is relevant for the neutrino flux. The flux-average procedure can include contributions from different kinematic regions where the neutrino flux has significant strength and processes other than direct one-nucleon emission can be important. Part of these contributions are recovered in the RGF model by the imaginary part of the ROP.

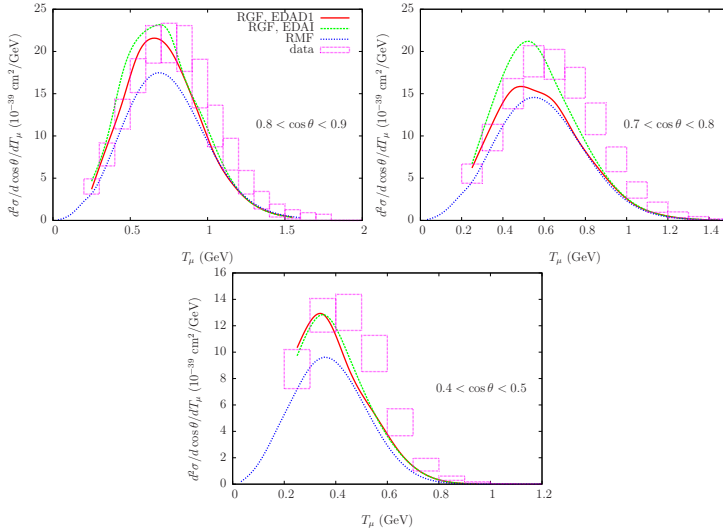


Figure 2. Flux-averaged double-differential cross section per target nucleon for the CCQE $^{12}\text{C}(\nu_\mu, \mu^-)$ reaction calculated in the RMF (blue line), the RGF-EDAD1 (red), and RGF-EDAI (green), and displayed versus T_μ for various bins of $\cos\theta$. In all the calculations the standard value of the nucleon axial mass, *i.e.*, $M_A = 1.03 \text{ GeV}/c^2$, has been used. Experimental data from [33].

The CCQE $^{12}\text{C}(\nu_\mu, \mu^-)$ cross sections measured by the MiniBooNE collaboration [33] have raised a strong debate over the role of the theoretical ingredients entering the description of the reaction. The experimental cross section is underestimated by the relativistic Fermi gas (RGF) and by other more sophis-

Relativistic Descriptions of Final-State Interactions in Quasielastic Electron and Neutrino-Nucleus Scattering

ticated models based on the IA unless the nucleon axial mass M_A is significantly enlarged with respect to the world average of all measured values ($1.03 \text{ GeV}/c^2$ [34, 35]), mostly obtained from deuteron data. The larger axial mass obtained from the MiniBooNE data on carbon can also be interpreted as an effective way to include medium effects which are not taken into account by the RFG and by other models based on the IA. Before drawing conclusions, the role of all nuclear effects must be carefully investigated.

In Figure 2 the flux-averaged RGF and RMF double-differential $^{12}\text{C}(\nu_\mu, \mu^-)$ cross sections are displayed as a function of the muon kinetic energy T_μ for various bins of $\cos \theta$, where θ is the muon scattering angle, and compared with the MiniBooNE data. The shape followed by both RMF and RGF results fits well the slope shown by the data. The RMF cross sections generally underpredict the data, the RGF results are generally larger than the RMF ones, in particular approaching the peak region, where the additional strength shown by the RGF produces cross sections in reasonable agreement with the data. The differences between the RGF-EDAI and RGF-EDAD1 results are in general of the order of the experimental errors.

The flux-averaged double-differential $^{12}\text{C}(\bar{\nu}_\mu, \mu^+)$ cross sections are shown in Figure 3 as a function of T_μ for four angular bins of $\cos \theta$, ranging from forward to backward angles. The RGF results are compared with the RPWIA and rROP ones and with the MiniBooNE data [36]. The rROP results are usually 15% lower than the RPWIA ones, both rROP and RPWIA generally underestimate the data. Larger cross sections, in better agreement with the data, are obtained with the RGF model, with both EDAD1 and EDAI. The differences between the RGF-EDAD1 and RGF-EDAI results are visible, although somewhat smaller than in the case of neutrino scattering.

The MiniBooNE Collaboration has also measured [37] the flux-averaged differential cross section as a function of the four-momentum transferred squared, $Q^2 = -q^\mu q_\mu$, for neutral-current elastic (NCE) neutrino scattering on CH_2 in a Q^2 range up to $\approx 1.65 \text{ (GeV}/c)^2$. The analysis of ν -nucleus NCE reactions introduces additional complications, as the final neutrino cannot be measured and a final hadron has to be detected: the cross sections are therefore semi-inclusive in the hadronic sector and inclusive in the leptonic one. The description of semi-inclusive NCE scattering with the RGF approach can recover important contributions that are not present in the RDWIA, which is appropriate for the exclusive scattering but neglects some final-state channels which can contribute to the semi-inclusive reaction. The RGF, however, describes the inclusive process and, as such, it may include channels which are not present in the semi-inclusive NCE measurements. In comparison with the MiniBooNE NCE data, the RDWIA generally underpredicts the experimental cross section while the RGF gives a reasonable agreement with the NCE data [21].

It is not easy to disentangle the role of contributions which may be neglected in the RDWIA or spuriously added in the RGF, in particular if we consider that both calculations make use of phenomenological ROP's. The comparison with

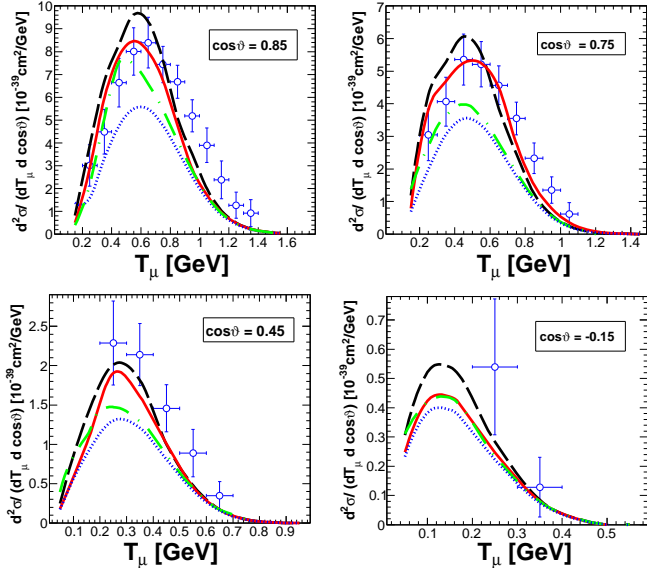


Figure 3. Flux-averaged double-differential cross section per target nucleon for the CCQE $^{12}\text{C}(\bar{\nu}_\mu, \mu^+)$ reaction as a function of T_μ for four angular bins of $\cos \theta$ calculated with the RGF-EDAD1 (solid lines) and the RGF-EDAI (dashed lines). The dotted lines are the rROP results calculated with the EDAD1 potential and the dot-dashed lines are the RPWIA results. Experimental data from [36].

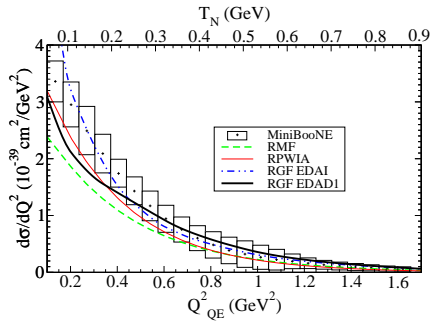


Figure 4. NCE flux-averaged ($\nu N \rightarrow \nu N$) cross section as a function of Q^2 calculated in the RPWIA (thin solid lines), RMF (dashed lines), RGF-EDAD1 (thick solid lines), and RGF-EDAI (dash-dotted lines). Experimental data from [37].

the results of the RMF model, where only the purely nucleonic contribution is included, can be helpful for a deeper understanding of FSI effects.

In Figure 3 the RMF, RGF, and RPWIA cross sections for NCE ($\nu N \rightarrow \nu N$) scattering are presented and compared with the experimental data. The variable $Q_{QE}^2 = 2m_N T$ is defined assuming that the target nucleon is at rest, m_N being

the nucleon mass and T the total kinetic energy of the outgoing nucleons. The RMF result has a too soft Q^2 behavior to reproduce the data at small Q^2 , while the RGF produces larger cross sections in better agreement with the data. The difference between the RGF-EDAD1 and RGF-EDAI results is significant. The RGF-EDAI cross section is in accordance with the shape and the magnitude of the data, while the RGF-EDAD1 one lies below the data at the smallest values of Q^2 considered in the figure. The RMF result gives the lowest cross section for low-to-intermediate values of Q_{QE}^2 .

4 Conclusions

A deep understanding of the reaction mechanism of neutrino-nucleus cross sections is mandatory for the determination of neutrino oscillation parameters. Reliable models are required where all nuclear effects are well under control. The RGF model has been discussed in this contribution. This model was originally developed for QE electron scattering, it has been tested in comparison with electron-scattering data, and it has then been extended to neutrino-nucleus scattering. In the RGF model FSI are described in the inclusive scattering by the same complex ROP as in the exclusive scattering, but the imaginary part redistributes and conserves the flux in all the channels. The RGF results are usually larger than the results of other models based on the RIA and can reproduce the CCQE MiniBooNE data without the need to increase the standard value of the nucleon axial mass. The enhancement of the RGF results is due to the translation to the inclusive strength of the overall effect of inelastic channels which are not incorporated in the RMF and in other models based on the IA. The use of phenomenological ROP's, however, does not allow us to disentangle different reaction processes and explain in detail the origin of the enhancement. The RGF results are also affected by uncertainties in the determination of the phenomenological ROP. A better determination which closely fulfills the dispersion relations deserves further investigation.

The relevance of contributions other than direct one-nucleon emission in kinematic regions where the experimental neutrino flux has significant strength has been confirmed by different studies [38–42]. Processes involving two-body currents, whose role is discussed in [43], should also be taken into account explicitly and consistently in a model to clarify the role of multinucleon emission.

Acknowledgements

We thank M.B. Barbaro, J.A. Caballero, F. Capuzzi, R. González-Jiménez, M.V. Ivanov, F.D. Pacati, and J.M. Udías for the fruitful collaborations which led to the results reported in this contribution.

Bibliography

- [1] S. Boffi, C. Giusti, and F.D. Pacati, *Phys. Rep.* **226** (1993) 1-101.

- [2] S. Boffi, C. Giusti, F.D. Pacati, and M. Radici *Electromagnetic Response of Atomic Nuclei* Oxford Studies in Nuclear Physics, Vol. 20, Clarendon Press, Oxford (1996).
- [3] J.M. Udías *et al.*, *Phys. Rev. C* **48** (1993) 2731-2739.
- [4] A. Meucci, C. Giusti, and F.D. Pacati, *Phys. Rev.C* **64** (2001) 014604-1-10.
- [5] A. Meucci, C. Giusti, and F.D. Pacati, *Phys. Rev.C* **64** (2001) 064615-1-8.
- [6] M. Radici, A. Meucci, and W.H. Dickhoff, *Eur. Phys. J. A* **17** (2003) 65-69.
- [7] C. Giusti *et al.*, *Phys. Rev.C* **84** (2011) 024615-1-12.
- [8] C. Maieron *et al.*, *Phys. Rev. C* **68** (2003) 048501-1-4.
- [9] J.A. Caballero *et al.*, *Phys. Rev. Lett.* **95** (2005) 252502-1-4.
- [10] J.A. Caballero, *Phys. Rev. C* **74** (2006) 015502-1-12.
- [11] F. Capuzzi, C. Giusti, and F.D. Pacati *Nucl. Phys.A* **524** (1991) 681-705
- [12] A. Meucci *et al.*, *Phys. Rev.C* **67** (2003) 054601-1-12.
- [13] F. Capuzzi *et al.*, *Ann. Phys.* **317** (2005) 492-529.
- [14] A. Meucci, C. Giusti, and F.D. Pacati *Nucl. Phys. A* **739** (2004) 277-290.
- [15] A. Meucci, C. Giusti, and F.D. Pacati *Nucl. Phys. A* **756** (2005) 359-381.
- [16] A. Meucci, C. Giusti, and F.D. Pacati, *Acta Phys. Polon. B* **37** (2006) 2279-2286.
- [17] A. Meucci, C. Giusti, and F.D. Pacati, *Acta Phys. Polon. B* **40** (2009) 2579-2584.
- [18] A. Meucci *et al.*, *Phys. Rev. C* **80** (2009) 024605-1-12.
- [19] A. Meucci *et al.*, *Phys. Rev. C* **83** (2011) 064614-1-10.
- [20] A. Meucci *et al.*, *Phys. Rev. Lett.* **107** (2011) 172501-1-5.
- [21] A. Meucci, C. Giusti, and F.D. Pacati, *Phys. Rev. D* **84** (2011) 113003-1-8.
- [22] A. Meucci, and C. Giusti, *Phys. Rev. D* **85** (2012) 093002-1-6.
- [23] A. Meucci *et al.*, *Phys. Rev. C* **87** (2013) 054620-1-14.
- [24] A. Meucci, C. Giusti, and M. Vorabbi, *Phys. Rev. D* **88** (2013) 013006-1-7.
- [25] R. González-Jiménez *et al.*, *Phys. Rev. C* **88** (2013) 025502-1-10.
- [26] Y. Horikawa, F. Lenz, and N.C. Mukhopadhyay, *Phys. Rev. C* **22** (1980) 1680-1695.
- [27] B.D. Serot and J.D. Walecka, *Adv. Nucl. Phys.* **16** (1984) 1-327.
- [28] E.D. Cooper *et al.*, *Phys. Rev.C* **47** (1993) 297-311.
- [29] E.D. Cooper *et al.*, *Phys. Rev.C* **80** (2009) 034605-1-5.
- [30] M. Anghinolfi *et al.*, *Nucl. Phys. A* **602** (1996) 405-422.
- [31] D.B. Day *et al.*, *Phys. Rev.C* **48** (1993) 1849-1863.
- [32] T. Leitner and U. Mosel, *Phys. Rev. C* **81** (2010) 064614-1-10.
- [33] A.A. Aguilar-Arevalo *et al.*, *Phys. Rev.D* **81** (2010) 092005-1-22.
- [34] V. Bernard, L. Elouadrhiri, and U.G. Meissner, *J. Phys.G* **28** (2002) R1-R35.
- [35] A. Bodek *et al.*, *Eur. Phys. J. C* **53** (2008) 349-354.
- [36] A.A. Aguilar-Arevalo *et al.*, *Phys. Rev.D* **88** (2013) 032001-1-31.
- [37] A.A. Aguilar-Arevalo *et al.*, *Phys. Rev.D* **82** (2010) 092005-1-16.
- [38] O. Benhar, P. Coletti, and D. Meloni, *Phys. Rev. Lett.* **105** (2010) 132301-1-4.
- [39] M. Martini *et al.*, *Phys. Rev. C* **81** (2010) 045502-1-5; *Phys. Rev. C* **84** (2011) 055502-1-7; *Phys. Rev. C* **87** (2013) 065501-1-5.
- [40] J. Nieves, I. Ruiz Simo, and M.J. Vicente Vacas, *Phys. Rev. C* **83** (2011) 045501-1-19; *Phys. Lett. B* **707** (2012) 72-75.
- [41] O. Lalakulich, K. Gallmeister, and U. Mosel, *Phys. Rev. C* **86** (2012) 014614-1-17.
- [42] A. Ankowski, *Phys. Rev. C* **86** (2012) 024616-1-13.
- [43] J.E. Amaro *et al.*, *Phys. Rev. D* **84** (2011) 033004-1-8.